

Role of Multiparametric Magnetic Resonance Imaging in Assessment of Different Renal Masses

Mohamed F. Abdel-Hamid^a, Ahmed F. Youssef^b, Hamada M. Khater^b

^a Department of Radiology,
Benha faculty of medicine,
Benha University, Egypt.

^b Department of Radiology,
Al-Ahrar Teaching Hospital,
Zagazig, Egypt.

Correspondence to:
Mohamed F. Abdel-Hamid,
Department of Radiology,
Benha faculty of medicine,
Benha University, Egypt.

Email:

mohamedfakhrymail@gmail.
com

Received: 5 April 2022

Accepted: 18 August 2022

Abstract

Background: Despite the fact that many fortuitous lesions have little metastatic potential, cross-sectional imaging is improving the diagnosis of renal tumours. **Purpose:** To assess the role of multiparametric magnetic resonance imaging (mpMRI) in the assessment of different renal masses. **Patients and Methods:** This was a cross-sectional study performed in in Benha university hospitals and was conducted on thirty eight patients having renal masses previously diagnosed with ultrasound and/or computed tomography, referred to the radiology, urology and oncology departments. All patients were subjected to full history taking, radiological examination including contrast enhanced MRI of the abdomen & pelvis and histopathological correlation of surgical specimens. **Results:** The percentage of benign and malignant cystic masses was 37%, whereas the percentage of benign and malignant solid masses was 63%. At b0 and b1000 s/mm², there was a significant statistical difference ($p > 0.05$) between the mean Analog to Digital Conversion (ADC) values of benign and malignant solid renal masses. Furthermore, at b0 s/mm², there was a statistically significant difference ($p > 0.01$) between the mean ADC values of benign and malignant cystic renal masses, and a statistically significant difference ($p > 0.05$) between the mean ADC values of benign and malignant cystic renal masses at b1000 s/mm². **Conclusion:** We confirmed the optimal diagnostic performance of mpMRI to identify benign and RCC in all clinical stages.

Keywords: mpMRI, renal, mass

Abbreviations:

mpMRI: Multiparametric magnetic resonance imaging; Analog to Digital Conversion (ADC); Renal tumour biopsy (RTB); renal cell carcinoma (RCC); gadolinium diethylenetriaminepentaacetic acid (Gd-DTPA); spin-echo echo-planar imaging (SE-EPI); Diffusion-weighted imaging (DWI); angiomyolipoma (AML); autosomal dominant polycystic kidney disease (ADPKD).

Introduction

With the increased use of radiological imaging modalities in recent years, the identification of renal masses has increased dramatically. Renal cell carcinomas represent the majority of renal masses, signifying 80 - 85% of primary renal malignancies and around 3% of adult tumours ⁽¹⁾.

Renal malignancies must be characterized in order to select the optimal therapy approach and enhance overall patient survival. Renal masses are being identified more frequently in clinical practice due to the growing use of high-resolution cross-sectional imaging. Consequently, accurate imaging characterization of these lesions is more crucial than before. Though, identifying appropriate imaging criteria for distinguishing between malignant and benign kidney tumours remains a challenge due to the vast range of imaging abnormalities reported as well as overlapping characteristics ⁽²⁾.

Renal tumour biopsy (RTB) can be used to get a pathological diagnosis for renal masses that aren't clear. The biopsy may not a trustworthy tool for tumour classification. RTB is also an invasive technique that can lead to consequences like bleeding, infection, pneumothorax, and hollow organ perforation. Novel imaging techniques are still helpful initial tools in the diagnosis and treatment ⁽³⁾.

The mpMRI based on numerous anatomic and functional factors plays a significant role in the identification and

characterization of renal masses and provides diagnostic value. MR imaging may help distinguish benign solid renal masses from many subtypes of renal cell carcinoma (RCC), as well as suggest a neoplasm's histologic grade and serve a key role in assuring adequate patient treatment to avoid unneeded interventions. It's also a good noninvasive imaging technique for patients under active monitoring for renal masses, as well as for follow-up following therapy ⁽⁴⁾. The MpMRI has been demonstrated to be useful in identifying cystic renal masses ⁽⁵⁾.

Purpose:

To assess the role of multiparametric magnetic resonance imaging (mpMRI) in the assessment of different renal masses.

Patients and Methods:

a. The current research was performed in a cross-sectional approach. The study was done in Benha university hospitals from July 2019 to May 2020 on thirty patients who had previously identified kidney masses using computed tomography and/or ultrasound and were sent to the oncology, radiology, and urology departments. The ages of patients ranged from 14 to 58 years old and included ten girls and twenty-eight males. The protocol for our study was approved by the institutional ethical committee. Patients were informed about the examination and gave their informed consent.

Patient inclusion criteria:

- Patients of any age and both sexes who had a kidney mass previously identified by CT scan or ultrasound were eligible for this research.

Patient exclusion criteria:

- Patients having inserted electronic and electric devices, insulin pumps, cardiac pacemakers, implantable intracranial metal clips, and hearing aids were all kept out from the research in addition to patient with renal impairment.

b. Scan protocol and parameters

Patients who fulfilled the inclusion criteria were assigned to the following procedures:

- History Taking - Personal information such as name, age, and gender. - A family history of comparable problems. - Medical history, including current symptoms, past tests, medical treatment, or previous surgical procedures.
- Upper abdomen contrast-enhanced MRI was the research approach. The MRI was performed using a superconductive magnet (1.5 Tesla) (General Electric SIGNA™ Creator, CHICAGO- United States). and a surface coil with respiratory triggering. A morphological study of the upper abdomen with four sequences was acquired prior to the acquisition of the functional DWI sequence:
 - axial T1-weighted turbo field echo (TFE)

- axial T2-weighted single-shot turbo spin echo (TSE)
- axial T2-weighted single-shot TSE with fat suppression [spectral selection attenuated inversion recovery (SPAIR)]
- Coronal T2-weighted single-shot TSE sequences.

The DWI functional study was carried out with a single shot spin-echo echo-planar imaging (SE-EPI) inversion mending sequence gained in the axial plane with sensitivity encoding (SENSE) in a solitary breath-hold through the following parameters:

- TR/TE 8000/58 ms
- EPI factor 53
- FOV/RFOV 320 mm / 100%
- Acquisition matrix 160 , reconstruction matrix 256
- 18 sections with a 7-mm slice thickness, interval 0 mm and two *b* values (0 & 1000 s/mm²)

Then a dynamic study was done with 3D isotropic fast-field echo (FFE) T1-weighted sequences with SPAIR fat-signal suppression in the axial plane subsequent to intravenous administration of 0.2 mmol/kg of 0.5 mol gadolinium-diethylenediamine pentaacetic acid (Gd-DTPA) contrast material by an injection rate of 2.0 ml/s, chased by 20 cc of saline solution with the same injection rate.

Table (1): Diffusion-weighted imaging (DWI) sequence parameters used for the magnetic resonance imaging study of kidneys and renal focal lesions

TR/TE	8000/58 ms
EPI factor	53
Thickness/interval	7.0/0.0 mm
Matrix (acq/rec)	160/256
FOV/RFOV	320/80%
b value	0 & 1000 mm ² /s
Scan length (s)	30
No. of sections	18

Qualitative and quantitative image analysis was carried out with the selection of regions of interest (ROIs) on the ADC map produced for each of the 18 slices gained on the basis of the algorithm signified by the following equation:

$ADC \text{ mm}^2/\text{s} = [1/1000 \times \ln (IS (b_0) / IS (b_1))]$, where $[IS (b_0) \text{ and } IS (b_1)]$ are the signal intensities obtained with two different b values (0 & 1000).

The mean and SD of ADC values for focal lesions with a maximum diameter less than 3 cm were measured using a single ROI, whereas those with a maximum diameter greater than 3 cm were measured using three ROIs of the same size, taking care to avoid sampling necrotic, hemorrhagic, calcified, and cystic areas.

The mean and standard deviation (SD) of the ADC value of the opposite kidney were calculated by drawing a single ROI of the same size and position in relation to the location of the contralateral lesion.

- **Histopathological assessment**

In patients with operable masses, the pathology results of the surgical specimen

(biopsy/partial nephrectomy/ total nephrectomy) were used to make the final diagnosis. For each patient, the findings obtained using mpMRI and DWI, including images, were correlated with the outcomes of histological findings and follow-up results.

Statistical analysis:

Our data was processed and analyzed using the IBM SPSS Statistics version 24.0 application (Armonk, USA). Frequencies and relative percentages were used to depict qualitative data. The Mann Whitney test was used to determine the difference between two sets of data that were not normally distributed. The Kruskal Wallis test (KW test) is used as a non-parametric variation of the F test when data does not follow a normal distribution. When P-value was $0 < 0.05$, the results were declared statistically significant. P-value $0. < 001$ was deemed highly statistically significant (HS), whereas P-value ≥ 0.05 was deemed statistically insignificant.

Results:

The highest age group impacted was 58 years old or older at 47.4% followed by

26.3% ranged from 47-58 then 15.7% ranged from 36-46 then 7.9% ranged from 25-35. Whereas the lowest age group impacted was 12-24 years old at 2.6% (**Fig.1a**). A total of 28 (73.6%) were males and 10 (26.3%) were females (**Fig. 1b**). The benign cases represented 34.2% while the malignant were 25 (65.8%) (**Fig. 1c**). Benign and malignant cystic masses denoted 37% while benign and malignant solid masses were 63% (**Fig.1d**).

In **Table 2** the angiomyolipoma (AML) represented the most frequent benign solid masses at 10.5% followed by oncocytoma at 5.3%. The least frequent masses were dromedary hump and metanephric adenoma at 2.6%. Renal cell carcinoma was the most prevalent kind of malignant solid mass in around 26.3 %, followed by renal secondaries in 13.3%. The lowest frequent masses were Wilms tumour and fibrosarcoma at 2.6%. Along with cystic masses, the most frequent cystic masses were the simple renal cyst (Bosniak I) of 13.1%, cystic renal cell carcinoma (Bosniak IV) of 7.8%, Multilocular cystic nephroma (Bosniak III) of 5.1%, autosomal dominant polycystic kidney disease (ADPKD), and nephric & perinephric abscess (Bosniak II &II f) of 2.6%.

All malignant solid renal masses exhibited bright signal intensity on DWI and low signal on ADC map (restricted diffusion) that appeared more clear at $b1000$ s/ mm^2 . There was a statistical significant difference between the signal intensities of all malignant solid renal masses on DWI at

$b0$ s/ mm^2 , no statistically significant difference presented between the signal intensities of all malignant solid renal masses on DWI at $b1000$ s/ mm^2 . Among the studied benign solid renal masses, there was a statistically significant difference ($p < 0.05$) between the mean ADC values of benign solid renal masses at $b0$ but there was no statistically significant difference ($p > 0.05$) between the mean ADC values of benign solid renal masses at $b1000$ s/ mm^2 . On other hand, among the studied cystic renal masses, There was no statistically significant difference between the mean ADC values of all categories t $b0$ and $b1000$ s/ mm^2 (**Table 3**).

There was a high statistically significant difference ($p < 0.05$) between the mean ADC values of benign and malignant solid renal masses at $b0$ & $b1000$ s/ mm^2 . Furthermore, there was a high statistically significant difference ($p < 0.01$) between the mean ADC values of benign and malignant cystic renal masses at $b0$ s/ mm^2 and a statistical significant difference ($p < 0.05$) at $b1000$ s/ mm^2 (**Table 4**). The cut-off values in the present study were less than or equal to (2.2 and 1.53×10^{-3} mm^2/sec for b values of 0 and 1000 sec/mm^2) for malignant solid masses and less than or equal to (2.2 and 1.6×10^{-3} mm^2/sec for b values of 0 and 1000 sec/mm^2) for malignant cystic masses. The sensitivity, specificity, and accuracy of multiparametric magnetic resonance imaging were 96.43%, 91.67%, 95% respectively (**Fig. 2**) compared to the histopathological diagnosis of the examined cases (**Table 5**).

Table (2): The histopathology of the investigated renal masses

Histopathology-based types	Investigated Population (N = 38)	
	Number	Percentage
Benign solid masses		
Oncocytoma	2	5.3%
AML	4	10.5%
Pseudomass (Dromedary hump)	1	2.6%
Metanephricadenom	1	2.6%
Malignant solid masses		
Renal cell carcinoma	(10)	26.3%
• clear cell RCC	7	
• Transitional RCC	2	
• Papillary RCC	1	
Wilmstumour	1	2.6%
FibroSarcoma	1	2.6%
Renal secondaries	(4)	10.5%
• lymphoma	1	
• leukemia	1	
• direct metastases	2	
Cystic masses		
Bosniak I	5	13.1%
Bosniak III	2	5.2%
ADPKD	1	2.6%
Multicystic dysplastic kidney	1	2.6%
Bosniak IV	3	7.8%
Bosniak II & II ^f *	1	2.6%

Table (3): Signal intensities of renal masses on diffusion weighted images

Final diagnosis	diffusion weighted images	ADC map	Mean ADC value b0 s/mm2 (x 10-3 mm2/s)	Mean ADC value b1000 s/mm2 (X 10-3 mm2/s)
Benign solid masses				
Onchocytoma	Bright	Low	1.29±0.70	0.78±0.68
Angiomyolipoma	Bright	Low	2.29 ±1.15	1.99±0.85
(AML)				
Pseudomass	Isointense	Isointense	3.13 ± 0.56	2.26±0.83
(Dromedary hump)				
Metanephricadenom	Bright	Low	3.31±1.05	2.35±0.83
P-Value			0.04*	0.06
Malignant solid masses				
Renal cell carcinoma				
clear cell RCC				
papillary RCC	Bright	Low	1.73± 0.63	1.8± 0.74
chromophobe RCC	Bright	Low	2.01±0.58	1.55±0.46
	Bright	Low	2.06±0.12	1.96±0.76
Wilms tumour	Bright	Low	2.67±0.76	1.68±0.29
Fibro Sarcoma	Bright	Low	2.31± 0.42	1.81±0.25
Renal secondaries				
• lymphoma	Bright	Low	1.15±0.34	0.82±0.21
• leukemia	Bright	Low	1.75±0.28	1.35±0.94
• direct metastases	Bright	Low	2.54±1.11	1.86±0.84
P-Value			0.03*	0.2
Cystic masses				
Category I	bright	Low	3.81±0.71	3.09±0.94
Category II& II _f	Intermediate	Intermediate	3.382± 1.04	2.32±1.17
Category III	Bright center & low septae	Lowcenter& brightseptae	2.826±0.89	2.93±1.21
Category IV	bright	Low	2.72±1.28	3.03±1.17
P-Value			0.4	0.6
Kruskal-Wallis Test*significant (p < 0.05)				

Table (4): The mean ADC values of benign and malignant renal masses

Renal Masses	ADC values ($\times 10^{-3} \text{ mm}^2/\text{s}$)	
	b = 0 s/mm ²	b = 1000 s/mm ²
Benign Solid	3.17±0.71	2.26±0.65
Malignant Solid	1.85± 0.92	1.01±0.62
P-Value	0.005**	0.003**
Benign Cystic	3.49 ± 0.97	2.82 ± 1.09
Malignant Cystic	2.22 ± 0.74	1.68 ± 0.43
P-Value	0.009**	0.02*

*significant (p < 0.05)

Table (5): The accuracy of mpMRI compared to histopathological diagnosis of the examined cases

Nature of the lesion	Imaging results	Histopathological and follow up results	sensitivity	Specificity	Accuracy
Benign	13	12	96.43%	91.67%	95%
Malignant	25	26			

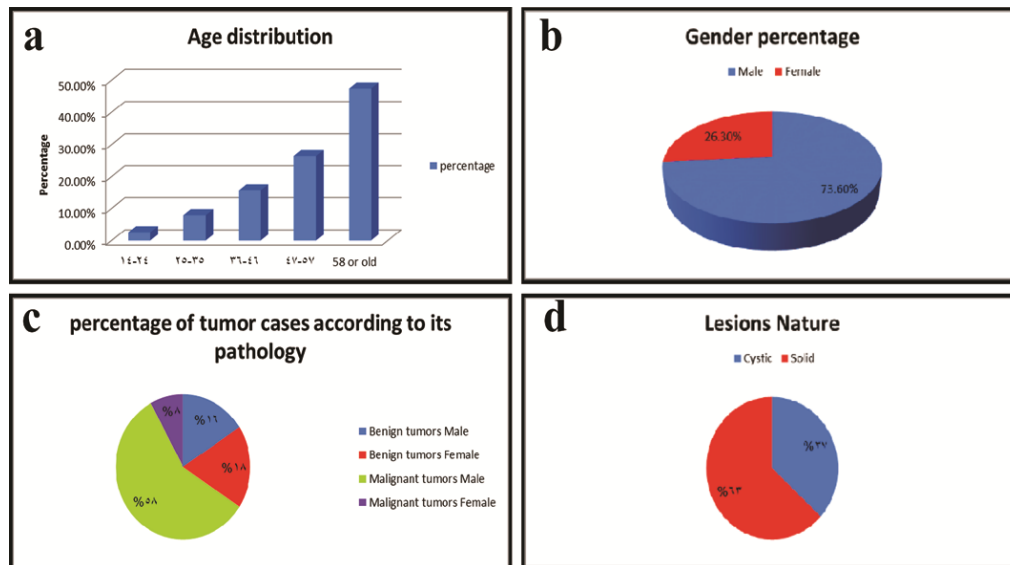


Fig. 1: A: Histogram showing sex distribution among the studied patients (N=38). B: The categorization of the examined renal masses is depicted as a pie chart. C: Percentage of tumour cases according to their pathology. D: Percentage of lesions nature done by multiparametric magnetic resonance imaging.

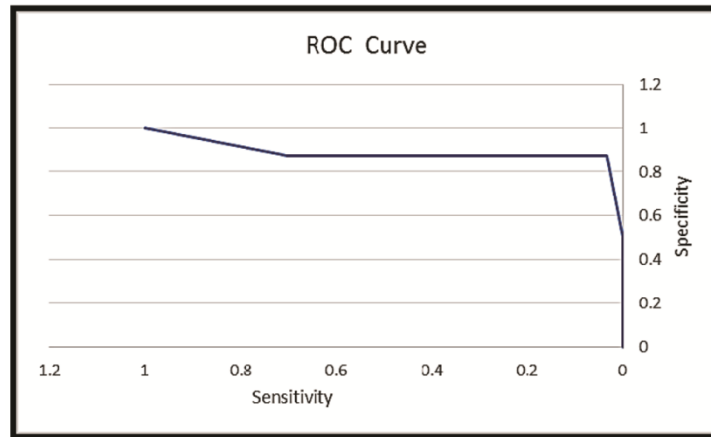


Fig. 2: Roc curve of mpMRI in assessment of different renal masses.

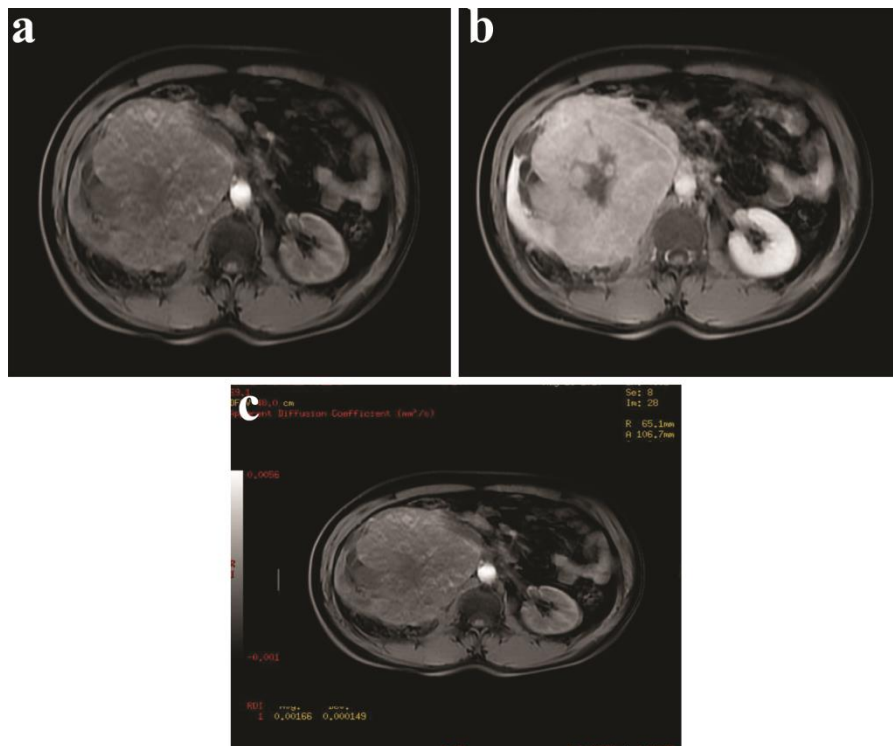


Fig. 3: Pathologically proved renal fibrosarcoma Large right solid renal mass. **(a):** showing mild heterogeneous contrast enhancement at the arterial phase. **(b):** with partial washout at the portal phase compressing on the renal pelvis exerting mild back-pressure changes. Encasing RT. renal artery & IVC with poor visualization of the anteriorly displaced right renal vein. **(c):** Showing diffusion restriction with ADC value = $1.6 \times 10^{-3} \text{ mm}^2/\text{s}$ keeping with malignant nature .

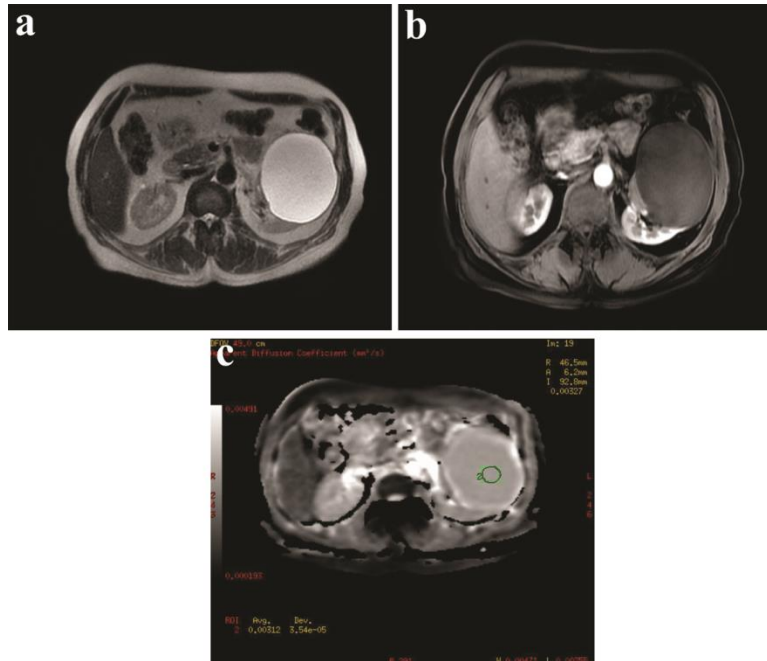


Fig. 4: Pathologically proved simple renal cyst. Left upper pole pure cystic renal mass displayed (a): high signal intensity at T2w , and (b): no contrast enhancement at the arterial phase. (c): ADC value = 3.1×10^{-3} mm²/s. (BOSNIAK 1) keeping with benign nature .

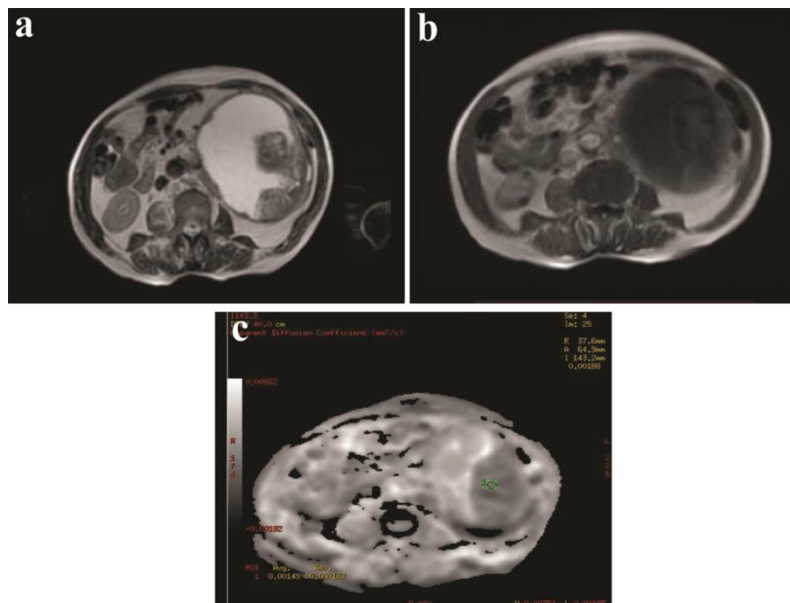


Fig. 5: Pathologically proved Cystic RCC. (a): Well defined left upper pole cystic renal mass with solid component displays intermediate signal at T2w. (b): and inhomogeneous contrast enhancement at the arterial phase. (c): Diffusion restriction at the ADC image ADC value = 1.4×10^{-3} mm²/s. (BOSNIAK IV) keeping with malignant nature .

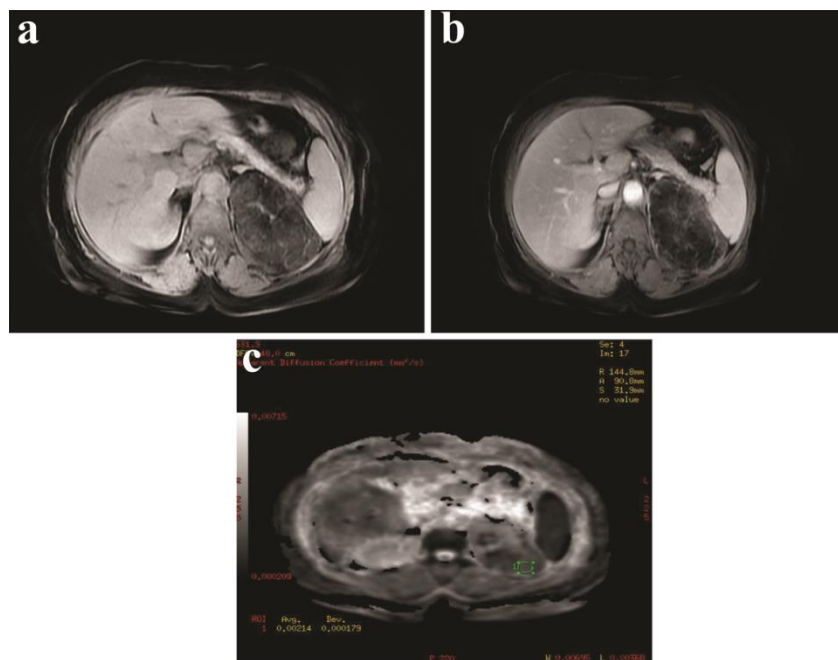


Fig. 6: Pathologically proved renal angiomyolipoma. (a): Well defined left upper renal polar solid lesion displaying fat signal intensity which is high in T1 WI, **(b):** moderate heterogeneous marginal and septal contrast enhancement at the arterial phase . **(c):** ADC value = 2.1×10^{-3} mm²/s keeping with benign nature.

Discussion:

Renal tumours that lacked macroscopic fat on imaging were formerly classified as renal cell carcinomas, regardless of size, requiring aggressive therapy. RMB was advised against because of concerns regarding tract seeding and diagnostic inaccuracy. It is critical to accurately examine renal masses to determine whether or not the tumors require surgical intervention (1). As medical imaging capabilities improve, evaluating imaging diagnostic powers may minimize the necessity for currently accessible, but invasive, procedures (e.g., RMB) (6). Multiparametric magnetic resonance imaging (mpMRI) offers a non-invasive, radiation-free characterization of renal masses to determine the RCC subtype. The present research aims to evaluate the role of

mpMRI in the assessment of different renal masses.

The most frequent benign solid masses in our research were angiomyolipomas (10.5%) followed by oncocytoma then pseudo mass, and metanephric adenoma. These results are in agreement with further study (7).

Renal cell carcinoma is the most frequent malignant solid mass accounting for 26.3% in our study followed by renal secondaries. The least frequent malignant solid masses were Wilms tumour, and fibrosarcoma as each accounted for 2.6%.

From a prognosis and management standpoint, accurate classification of RCC histological subtypes is critical. In this

study, the RCC is the most common subtype (70%) of total renal cell carcinoma that has a worse prognosis than papillary RCC (20%), with chromophobe RCC (10%). Our results are inconsistent with Van Oostenbrugge study⁽⁷⁾ who verified that the most common kinds of RCC were the clear cell RCC followed by papillary RCC then chromophobe RCC subtypes. Moreover, these results were verified⁽⁸⁾.

Characterization of renal tumours is essential for determining the appropriate therapy strategy and improving overall patient survival⁽²⁾. In this study, there were statistically significant difference ($p < 0.05$) between different types of solid renal masses. Our findings are consistent with another study⁽⁹⁾, which discovered a substantial difference in the mean ADC between different kinds of malignant RCC but not between different types of benign renal masses. The disagreement with our results by another study⁽¹⁰⁾ may be due to different sample sizes, b values, coil systems, breath-hold versus free breathing, and field strengths used for MRI. Renal lymphoma tends to show diffusion restriction⁽¹¹⁾. In these series, one lesions was easily seen with high signal on DWI. They had the lowest ADC values among all malignant lesions. These results are in agreement with other study⁽¹²⁾.

All solid renal masses exhibits bright signal intensity on DWI and low signal on ADC map (restricted diffusion) that appears more clear at $b1000 \text{ s/mm}^2$. There is a statistically significant difference between the signal intensities of all malignant solid renal masses on DWI at $b \text{ 0s/mm}^2$ but there is no

statistically significant difference between the signal intensities of all malignant solid renal masses on DWI at $b1000\text{s/mm}^2$. These findings show that DW imaging has the potential to be useful in the characterization of renal masses. Because of their increased cellularity, most solid tumors demonstrated limited diffusion, resulting in restricted water movement and high signal intensity on DWI⁽⁹⁾. The mean ADC of RCC is much less than the elevated ADC of renal cysts (**Fig. 3**), which is consistent with the findings of another study⁽¹³⁾.

In our study, the highest ADC value of all lesions was that of a simple renal cyst (**Fig 4**). This could be attributed to their fluid content, with the non-restricted motion of water molecules⁽¹⁴⁾. Our findings were in concordance with previous reports (13). The mean ADC value of benign cystic lesions is higher than that of cystic RCCs (**Fig 5**). This finding is particularly useful in diagnosing cases in which gadolinium cannot be given or the contrast bolus is suboptimal, leading to difficulty in identifying an enhancing mural nodule. Repeated measurements of all regions of a cystic tumour, particularly of the peripheral regions showing nodularity, may determine the malignant potential of a cystic mass. These results are in agreement with another study⁽¹⁵⁾ which verified ours.

In our study, a statistically significant difference ($p < 0.05$) was obtained between the mean ADC values of benign solid renal masses at $b0$ while there was no statistically significant difference ($p > 0.05$) between the mean ADC values of benign solid renal masses at $b1000 \text{ s/mm}^2$. The mean ADCs in AMLs was lower than the RCCs (**Fig 6**).

These results are inconsistent with other studies^(15 and 16). The mean ADC value of oncocytoma was higher than RCC as two cases of oncocytoma were diagnosed and displayed low signal intensity on DWI at $b1000s/mm^2$, bright SI on ADC map. Other research⁽¹⁷⁾ verified that ADC values of malignant tumours were relatively lower than those of benign tumours because of the higher cellularity and smaller extracellular space of malignant tumours. Other study⁽¹⁸⁾ assured these results. In contrast to our results, other researchers⁽¹⁹⁾ stated that similar ADCs can be seen with oncocytomas and clear cell RCC. The difference may be attributed to the hardware and software related issues, such as field in homogeneity, methodological, coil systems, and intrinsic physical factors related to the differences in the design of the DWI sequences. The mean ADC value of cystic RCCs was higher than that of clear type RCCs. Papillary RCC of solid nature, although being hypovascular, it displayed only mild enhancement at the nephrographic phase, it displayed slightly higher ADC value compared with solid clear type RCC. Our results are consistent with other researches^(20 and 21).

There was a high statistically significant difference ($p < 0.05$) between the mean ADC values of benign and malignant solid renal masses at $b0$ & $b1000 s/mm^2$. Furthermore, there was a high statistically significant difference ($p < 0.01$) between the mean ADC values of benign and malignant cystic renal masses at $b0 s/mm^2$ and a statistical significant difference ($p < 0.05$) at $b1000 s/mm^2$. Many researchers have reported an increased

diagnostic value when using DWI for tumour differentiation in the differential diagnosis of cerebral tumours⁽²²⁾ as well as in the characterization of focal liver lesions and many other body organs⁽²³⁾.

The sensitivity, specificity, and accuracy of multiparametric magnetic resonance imaging were 96.43%, 91.67%, 95% respectively compared to histopathological diagnosis of the examined cases. This difference may be attributed to some different studied varieties like (fibrosarcoma, leukemia, Wilms, multilocular cystic nephroma and others). Also, we studied the solid and cystic masses as two separate entities in contrast to other researchers⁽¹⁵⁾ who studied the benign and malignant masses as a whole.

Conclusion:

Recognizing the most essential imaging findings of solid renal tumours can help with diagnosis and treatment. As a noninvasive imaging tool, multiparametric MR imaging gives crucial information that can aid in the distinction of the most common renal masses, including common RCC subtypes and AMLs, and therefore may contribute to the selection of the most suitable management and follow-up of these lesions. Breath-hold DW imaging could be easily added to a routine renal MR imaging protocol, it is an accurate method for renal lesion characterization, and can yield useful information additional to that acquired with contrast-enhanced MR imaging. We recommend using high b values for better results.

References

1. Agnihotri S, Kumar J, Jain M, Kapoor R, Mandhani A. Renal cell carcinoma in India demonstrates early age of onset & a late stage of presentation. *The Indian journal of medical research*. 2014; 140(5): 624-629.
2. Lopes Vendrami C, Parada Villavicencio C, DeJulio TJ, Chatterjee A, Casalino DD, Horowitz JM et al. Differentiation of solid renal tumors with multiparametric MR imaging. *Radio Graphics*. 2017; 37(7):2026–2042.
3. Blumenfeld AJ, Guru K, Fuchs GJ, Kim HL. Percutaneous biopsy of renal cell carcinoma underestimates nuclear grade. *Urology*. 2010; 76(3): 610–613. <https://doi.org/10.1016/j.urology.2009.09.095>.
4. Ramamurthy NK, Moosavi B, McInnes MD, Flood TA, Schieda N. Multiparametric MRI of solid renal masses: pearls and pitfalls. *Clin Radiol*. 2015; 70(3):304–316.
5. Ferreira AM, Reis RB, Kajiwara PP, Silva BE, JR EJ, Muglia FV. MRI evaluation of complex renal cysts using the Bosniak classification: a comparison to CT. *Abdom Radiol*. 2016; 41: 2011–2019.
6. Bindayi A, Hamilton ZA, McDonald ML, Yim K, Millard F, McKay R, et. al. Neoadjuvant therapy for localized and locally advanced renal cell carcinoma. *Urol Oncol*. 2018; 36(1):31–37.
7. VanOostenbrugge TJ, Fütterer JJ, Mulders PF. Diagnostic imaging for solid renal tumors: a pictorial review. *Kidney Cancer*. 2018; 2(2):79–93.
8. Johnson BA, Kim S, Steinberg RL, de Leon AD, Pedrosa I, Cadeddu JA. Diagnostic performance of prospectively assigned clear cell Likelihood scores (ccLS) in small renal masses at multiparametric magnetic resonance imaging. *Urol Oncol*. 2019; 37(12):941–946.
9. El-Sayed AM, Abd-elaziz IM, Salem AF, Alaa Eldin AM. Added Value of Apparent Diffusion Coefficient and Diffusion Weighted Imaging in Characterization of Renal Masses. *Annals of R.S.C.B*. 2021; 25 (6):15004-15013.
10. Manenti G, Di Roma M, Mancino S, Bartolucci DA, Palmieri G, Mastrangeli R, et. al. Malignant renal neoplasms: correlation between ADC values and cellularity in diffusion weighted magnetic resonance imaging at 3 T. *Radiol Med*. 2008; 113: 199–213.
11. Ganeshan D, Iyer R, Devine C, Bhosale P, Paulson E. Imaging of primary and secondary renal lymphoma. *Clin Radiol*. 2013; 68: 224-231.
12. Zhang Y, Chen J, Shen J, Zhong J, Ye R, Liang B. Apparent diffusion coefficient values of necrotic and solid portion of lymph nodes: differential diagnostic value in cervical lymphadenopathy. *Clin Radiol*. 2013; 68(3):224-31. doi: 10.1016/j.crad.2011.04.002.
13. Inci E, Hocaoglu E, Aydin S, Cimilli T. Diffusion weighted magnetic resonance imaging in evaluation of primary solid and cystic renal masses using the Bosniak classification. *Eur J Radiol*. 2012; 81:815–20.
14. Kilickesmez O, Inci E, Atilla S, Tasdelen N, Yetimo B, Yencilek F, et al. Diffusion-weighted imaging of the renal and adrenal lesions. *J Comput Assist Tomogr*. 2009; 33 (6): 828-833.
15. Doganay S, Kocakoc E, Aglamis S, Akpolat N, Orhan I. Ability and utility of diffusion-weighted MRI with different b values in the evaluation of benign and malignant renal lesions. *Clin Radiol*. 2011; 66: 420-425.
16. Sandrasegaran K, Sundaram CP, Ramaswamy R, Akisik FM, Rybberg MP, Lin Cet al. Usefulness of diffusion-weighted imaging in the evaluation of renal masses. *AJR Am J Roentgenol*. 2010; 194: 438 – 45.
17. Lassel EA, Rao R, Schwenke C, Schoenberg SO, Michaely HJ. Diffusion-weighted imaging of focal renal lesions: a meta-analysis. *Eur Radiol*. 2014; 24: 241–249.
18. Taouli B, Thakur RK, Mannelli L, Babb JS, Kim S, Hecht EM, et al. Renal lesions: characterization with diffusion-weighted imaging versus contrast-enhanced MR imaging. *Radiology*. 2009; 251: 398-407.
19. Hötter AM, Karlo CA, Zheng J, Moskowitz CS, Russo P, Hricak H, Akin O. Clear Cell Renal Cell Carcinoma: Associations Between

- CT Features and Patient Survival. American Journal of Roentgenology. 2016; 206(5) <https://www.ajronline.org/doi/10.2214/AJR.15.15369>
20. Squillaci E, Manenti G, Di Stefano F, Miano R, Strigari L, Simonetti G. Diffusion-weighted MR imaging in the evaluation of renal tumors. J Exp Clin Cancer Res. 2004; 23: 39–45.
21. Zhang Y, Jay Schauer J, Zhang Yu, Zeng L, Wei Y, Yuan Liu, Shao M. Characteristics of Particulate Carbon Emissions from Real-World Chinese Coal Combustion. Environ. Sci. Technol. 2008; 42 (14): 5068–5073. <https://doi.org/10.1021/es7022576>
22. Svolos P, Kousi E, Kapsalaki E, Theodorou K, Fezoulidis I, Kappas C, Tsougos I. The role of diffusion and perfusion weighted imaging in the differential diagnosis of cerebral tumors: a review and future perspectives. Cancer Imaging. 2014; 14(1):20.
23. Okasha A, Wagdy W, Wahman M, Rabea H. Role of diffusion weighted magnetic resonance imaging in diagnosis of hepatic focal lesions. World J Gastroenterol. 2018; 14(46):5805–5812.

To cite this article: Mohamed F. Abdel-Hamid, Ahmed F. Youssef, Hamada M. Khater. Role of Multiparametric Magnetic Resonance Imaging in Assessment of Different Renal Masses. BMFJ 2023;40 (Radiology):70-84.